The Hydrolysis of Chlorine Nitrate on Ice Is Autocatalytic

Franz M. Geiger, Charles D. Pibel,† and Janice M. Hicks*

Department of Chemistry, Georgetown University, Washington, D.C. 20057

Received: December 31, 2000; In Final Form: March 23, 2001

A key chemical reaction in stratospheric ozone depletion is the reaction of chlorine nitrate ($ClONO_2$) with water. This reaction is known to be catalyzed in the presence of ice particles found in polar stratospheric clouds (PSCs). However, the mechanism and time scale of the reaction, and the role of the ice surface, are not well understood. This surface second harmonic generation study shows that the submonolayer $ClONO_2$ hydrolysis on basal ice (Ih) surfaces at 185 K occurs autocatalytically, with the product molecule HOCl acting as the autocatalyst. The other product, HNO_3, acts to delay the reaction. The hydrolysis reaction is surprisingly slow, with induction times that range from 100 to 1000 s, depending upon how much reactant is initially present. It is proposed that the ice surface serves as a reservoir, enabling the reaction to be acid catalyzed.

1. Introduction

In the past decade there has been intense work on the chemistry of stratospheric ozone depletion, which is now known to be catalyzed by icy particulates. While many studies have focused on the role of the solids in this chemistry, the mechanisms of the key reactions and their time scales are not yet clear. In this work, a surface-sensitive laser method is utilized to explore the hydrolysis of chlorine nitrate ($ClONO_2$) to hypochlorous acid (HOCl) and nitric acid (HNO_3) on single crystalline basal ice surfaces under pressure and temperature conditions representative of the stratosphere. This work contributes to an understanding of the surface chemistry of ice, which is surprisingly not yet well characterized.

$ClONO_2$, HOCl, and hydrochloric acid (HCl) are thought to be culprits in key chemical reactions that lead to stratospheric ozone depletion.[1−3] The following reactions have been proposed for these species adsorbed on polar stratospheric cloud particles consisting of ice (type II) and nitric acid hydrates (NAH, type I):

$$ClONO_2(g) + H_2O(s) \rightarrow HNO_3(ad) + HOCl(ad) \quad (1)$$

$$ClONO_2(g) + HCl(ad) \rightarrow Cl_2(g) + HNO_3(ad) \quad (2)$$

$$HOCl(g) + HCl(ad) \rightarrow Cl_2(g) + H_2O(s) \quad (3)$$

Reactions 1−3 correspond to the heterogeneous production of active chlorine and lead to the denitrification of the stratosphere.[1,4,5] As a result, ozone is effectively depleted by radical reactions.[1−5] PSCs form below 195 K, temperatures which are reached inside the stratospheric polar vortex above Antarctica and the Arctic.[6,7] Due to their small size (1−10 μm) and slow growth under near equilibrium conditions, PSC particles are thought to be single crystalline,[8,9] with low index faces exposed.[10] In the case of hexagonal ice Ih, these are the basal (0001) and prism (1100) faces.[11]

Various studies have probed reactions 1−3 using flow tube reactors,[12−15] Knudsen cell methods,[16,17] and ultrahigh vacuum techniques[18] using vapor-deposited ice and NAH. The kinetic analysis using these methods can be complicated,[19] and the ice is often difficult to characterize.[20] While these studies have shown that in contrast to the gas-phase reactions, chlorine activation does take place in the presence of ice via reactions 1−3, not much is known about the reaction rates, the reaction mechanism, or why ice is required to catalyze the reaction.

One of the difficulties in studying ice from a surface science point of view is its high vapor pressure: at 185 K the equilibrium vapor pressure is 10^{-4} Torr, precluding many traditional surface science approaches that typically require $<10^{-6}$ Torr pressures. One suitable method with demonstrated surface selectivity and sensitivity is the nonlinear optical method, second harmonic generation (SHG).[21,22] SHG provides an in-situ, on-surface direct probe of the surface chemistry of ice.[23−26]

In SHG, two photons of a single frequency are concertedly transformed into one photon at double the frequency. This nonlinear optical scattering effect becomes important when high-intensity light fields (e.g., from pulsed lasers) are present in noncentrosymmetric media, including surfaces.[21] The effect originates from the second-order nonlinear susceptibility $\vec{\chi}^{(2)}$ of the surface molecules which, for small coverages, is modeled as the product of the number density of the molecules adsorbed on a surface (N_s) and the molecular hyperpolarizability, averaged over all orientations $\langle\vec{\alpha}^{(2)}\rangle$. The square root of the SHG intensity is proportional to $\vec{\chi}^{(2)}$ and hence the number density of adsorbates at the surface

$$\sqrt{I_{2\omega}} \propto \vec{\chi}^{(2)} = N_S \cdot \langle\vec{\alpha}^{(2)}\rangle \quad (4)$$

In molecular surface systems, the SHG signal is thought to originate over the spatial dimension of just one or a few monolayers.[22,24]

The SHG scattering intensity is enhanced whenever the second harmonic frequency is in resonance with the adsorbed molecule.[21] Thus, by scanning laser wavelengths, SHG can be utilized for obtaining nonlinear electronic spectra on the surface.

* To whom correspondence should be addressed. (hicksj@georgetown.edu).
† Department of Chemistry, American University, Washington, DC.

10.1021/jp0101007 CCC: $20.00
Published on Web 04/25/2001

A second feature of this study is that single crystalline ice is used, with the basal face exposed, and held at equilibrium with its vapor pressure at all temperatures used in the experiment.

2. Experimental Section

The experimental apparatus has been described.[23−26] Single crystalline ice is grown using an adaptation of the Bridgeman technique, and its crystallinity is verified using polarizing microscopy.[26] A 3 mm thick piece of 1 cm diameter is cleaved from the crystal sample, such that the basal plane (0001) is exposed, and frozen onto a cold polished aluminum sample mount that is in thermal contact with a liquid nitrogen dewar serving as the sample holder. A chromel−alumel thermocouple is embedded in the ice. The sample holder is placed into a turbo-pumped (170 L/s) Pyrex glass vacuum chamber with a base pressure of 10^{-8} Torr. A ceramic button heater (Spectra-Mat E−292) connected to the sample mount allows for temperature regulation of the ice crystal between 110 and 270 K via a temperature controller. The crystal is annealed at 190 K for 30 min. During the experiments, the surface of the crystal is maintained in equilibrium with the surrounding water vapor[27] by additional dosing of water. Water and the sample gases are admitted to the chamber using Chemglass Teflon leak valves. Partial pressures are measured using a quadrupole mass spectrometer (Ametek Dykor MA200 M), and the total pressure inside the chamber is determined via a calibrated Bayard-Alpert ionization gauge (Granville Phillips).

The laser fundamental is the 600 nm output of a pulsed 4 MHz cavity-dumped subpicosecond dye laser (Rhodamine-6G, tunable from 580 to 620 nm, 100 mW average power) pumped by a picosecond Nd:YAG laser (Spectra Physics 3800S). The beam is focused on the ice sample to approximately 30 μm. The laser is directed at the ice surface at a 60° angle, and collinear with the linear reflection is the SHG signal. Both the reflected fundamental and second harmonic light pass through a fused quartz window. The SHG light is then separated from the fundamental frequency by two Corning 7-54 filters, and its polarization is analyzed using a quartz Rochon polarizer. The SHG light is further separated from the fundamental frequency by a monochromator and detected by single photon counting techniques. The signal is normalized to the laser intensity by a reference SHG signal generated in transmission through potassium dihydrogen phosphate (KDP) powder in an index-matched fluid. The reference signal is collected using a detection system identical to the one used in the sample line, correcting for the wavelength response of the detection system.

$ClONO_2$ is prepared from N_2O_5 and Cl_2O (see safety precautions in ref 24). HNO_3 is dosed from the vapor phase of a 69% nitric acid solution (EM Science) placed in an evacuated 250 mL sample flask. HOCl is prepared by hydrolysis of $ClONO_2$ in 40% sulfuric acid (EM Science).[24] Using low partial pressures of the sample gases $ClONO_2$, HOCl, and HNO_3 (10^{-9} to 10^{-8} Torr) and exposure times ranging from 10 to 300 s, exposures of 0.1 up to 3 langmuirs are achieved with a reproducibility of 10%.

We have previously reported that the SHG response from a clean ice surface is constant over the wavelength range of the dye laser (580−640 nm), yielding five SHG photons per second with our dye laser system.[25] When the ice surface is probed with the s-in/s-out polarization combination (the s-in/s-out polarization combination is given by probing the surface with light polarized parallel to the surface and detecting only the component of the SHG that is polarized parallel to the surface as well), a nonzero SHG signal is obtained, which is consistent with the 3*m* symmetry of the crystalline basal plane of ice.[24] In other studies, we showed that SHG signals from HOCl adsorbed to ice are resonantly enhanced and therefore provide a surface selective signature for probing reaction 1.[23,24] Addition of HOCl on the ice surface also causes an increase in the s-in/s-out signal, consistent with increased hyperpolarizability, and further, indicating that these molecules are adsorbed in registry with the underlying ice lattice.[24]

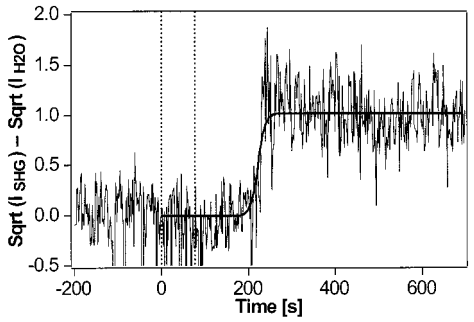

Figure 1. SHG signal at 300 nm recorded vs time after exposing the ice crystal held at 181 K to 0.4 langmuir $ClONO_2$. 1 langmuir = 10^{-6} Torr·s and corresponds to monolayer coverage if the sticking coefficient of the adsorbate is unity. The solid line is the best fit to eq 5. The surface was probed with light plane polarized at a 45° angle from the surface and collecting only light polarized parallel to the surface (s).

3. Results

When the clean ice surface is exposed to a submonolayer dose of $ClONO_2$, a significant time delay is observed before the SHG signal increases sigmoidally. This is shown in Figure 1, where the ice held at 181 K was exposed to 0.4 langmuir $ClONO_2$. The partial pressure of $ClONO_2$ was 5×10^{-9} Torr. Exposure started at 0 s and lasts for 80 s, and the dosing block is indicated by the dashed vertical bars. This signal increase is due to the formation of HOCl, which was verified by taking a surface SHG spectrum after the increased SHG signal was stable over time.[24] Also, exposing excess HCl to the surface after the increased SHG signal was stable caused an exponential decay of the signal following pseudo-first-order kinetics, indicating that reaction 3 was taking place.[24] Other control experiments show that the SHG signal increase is not due to coproduct HNO_3:[24] exposure of the clean ice surface to HNO_3 did not result in an SHG signal change. This is expected since HNO_3 does not have an electronic transition at 300 nm and resonance enhancement such as for HOCl does not occur.

On the basis of the similar UV absorption cross sections of $ClONO_2$ and HOCl around 290 and 300 nm, respectively,[20] resonant enhancement of the SHG signal would also be expected for $ClONO_2$. However, even when probing the ice surface with laser light at 580 nm and recording the second harmonic signal at 290 nm, no increase of the signal was observed during $ClONO_2$ exposure. This lack of signal increase could be because the electronic structure of $ClONO_2$ adsorbed at the ice surface is different from the electronic structure of gaseous $ClONO_2$; it may be altered in such a way that the electronic resonance is shifted out of the wavelength range of our dye laser. This could be due to hydration of $ClONO_2$ at the surface. Another possibility is that $ClONO_2$ adsorbs dissociatively on the ice surface. This latter picture is supported by ab initio calculations showing that as the size of a water cluster is increased, an attached $ClONO_2$ molecule becomes increasingly polarized along the Cl−O bond.[28] We also preconditioned the ice crystal held at 173 K with HCl and exposed the surface to $ClONO_2$, but formation of HOCl was not observed, indicating that at that

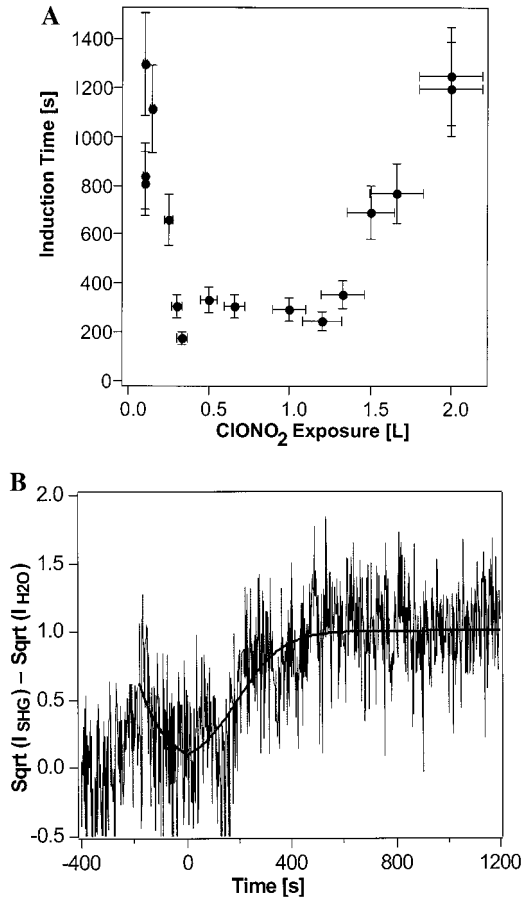

Figure 2. (A) Induction times for $ClONO_2$ hydrolysis on ice held at 173 K and various $ClONO_2$ exposures between 0.1 and 2.0 langmuirs. The induction times are the times from starting exposure to the inflection point of the SHG vs time trace and were calculated from eq 5. Errors in the induction times are obtained by propagating the errors associated with fit parameters n and r in eq 5. Errors in the $ClONO_2$ exposure are based on the 10% reproducibility of $ClONO_2$ exposure. (B) SHG signal recorded vs time for ice held at 173 K. The initially clean ice was preexposed to 0.1 langmuir HOCl at negative times. The solid line before zero time is the best fit to a single exponential of the form $a\ e^{-bt}$; after zero time it is the best fit to eq 5.

temperature, reaction 2 was dominant. This is consistent with the finding by Oppliger et al.[17] Despite its electronic resonance at around 300 nm, Cl_2 is not seen at the surface. This is consistent with the finding by Banham et al.[29] that Cl_2 has a temperature of maximal desorption of 110 K.

We characterize the SHG vs time traces by fitting the normalized SHG traces to the following sigmoidal fit function:

$$\sqrt{I} - \sqrt{I_{H_2O}} = \frac{1}{1 + n\, e^{-r\,t}} \qquad (5)$$

The left-hand side of the equation represents the square root of the SHG signal with the background originating from the clean ice surface subtracted; n and r are fit parameters. The SHG vs time trace in Figure 1 can thus be understood to represent the degree to which HOCl has been formed: at early times, very little HOCl is formed; at late times, the maximal amount of HOCl has been formed. The induction times are characterized by $\tau = \ln(n)/r$ and correspond to the time τ at which the signal intensity has reached its half-maximum. When measuring the induction times for various $ClONO_2$ exposures between 0.1 and 2.0 L, we find that they vary with the amount of $ClONO_2$ exposed to the surface. This is shown in Figure 2A, where it can be seen that the induction times decrease initially and then increase again with increasing $ClONO_2$ exposure above 1.33 langmuirs.

The sigmoidal shape of the time evolution of HOCl (Figure 1) and the behavior of the induction times (Figure 2A) are indicative of an autocatalytic process, in which one of the product acids (either HNO_3 or HOCl) increases the rate of further $ClONO_2$ hydrolysis. Autocatalysis is a well-studied phenomenon[30] with examples in many biological and chemical systems. A standard test for autocatalysis is to start the reaction in the presence of the autocatalyst, which will shorten the induction times. We performed this test first on the product acid HNO_3 by exposing 0.4 langmuir $ClONO_2$ to ice surfaces that had been preconditioned with various amounts of HNO_3 (0.1−0.5 langmuir). Fits to eq 5 yielded induction times that *increased* linearly with HNO_3 preexposure at $12(2) \times 10^2$ seconds per langmuir of exposed HNO_3. This lengthening effect of HNO_3 on the induction times clearly shows that HNO_3 does not play an autocatalytic role in the heterogeneous hydrolysis reaction of $ClONO_2$. Rather, it serves as an inhibitor, poisoning the reaction. This result is consistent with previous work by others showing that the $ClONO_2$ hydrolysis reaction occurs less efficiently on NAH surfaces.[12−17]

When the other product acid, namely HOCl, is dosed onto the ice prior to $ClONO_2$ exposure, the induction times to the onset of HOCl production are found to be shortened considerably. This is shown in Figure 2B, where the HOCl predosing experiment is performed in the following way: at negative times, the SHG signal increases upon admission of HOCl (0.1 langmuir exposure). Once the HOCl valve is closed, the SHG signal decays over time as HOCl desorbs from the ice surface, consistent with our earlier studies of HOCl desorption from ice.[24] At 0 s, the ice surface was exposed to 2.0 langmuirs $ClONO_2$ (partial pressure $= 7 \times 10^{-8}$ Torr for 30 s), resulting in an increase of the SHG signal after an induction time of about 200 s. The 200 s induction time obtained in this test for the hydrolysis of $ClONO_2$ on ice is 5 times shorter than the induction time obtained when the clean ice surface is exposed to the same amount of $ClONO_2$. The shortening effect that HOCl has on the induction times clearly shows that the HOCl product acid acts as an autocatalyst in the heterogeneous hydrolysis reaction of $ClONO_2$.

If one considers the SHG intensity after the plateau has been reached in traces such as shown in Figure 1 as a function of $ClONO_2$ exposure, one obtains Langmuirian behavior. This is shown in Figure 3A, where the relative HOCl coverage was determined by measuring the plateau SHG intensity after the $ClONO_2$ hydrolysis is complete. This SHG yield is normalized to the maximal SHG yield (∼30 photons per second at 300 nm) and is plotted vs $ClONO_2$ exposure up to 2.0 langmuirs (background from the clean ice surface subtracted). Up to about 1.0 langmuir $ClONO_2$ exposure, the HOCl yield increases with $ClONO_2$ exposure, while it remains constant for higher exposures. Insofar as the SHG signal from HOCl reports on the initial adsorption of $ClONO_2$, then these data indicate the $ClONO_2$ adsorption on ice is Langmuirian.

The effect of increasing the $ClONO_2$ concentration on the reaction can be seen in Figure 3B. It can be seen that for $ClONO_2$ exposures up to 0.5 langmuir, the concomitant increase in HOCl coverage speeds up the hydrolysis rate. A simple one-step autocatalysis model was employed to obtain the autocatalytic reaction rates. For an autocatalytic reaction such as $A + P \xrightarrow{k} P(2P)$ the following time dependence is obtained for the product concentration:[30]

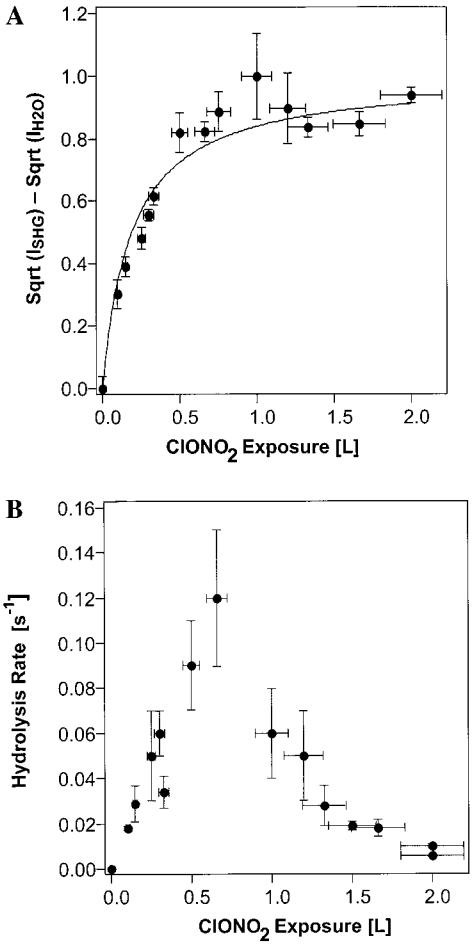

Figure 3. (A) SHG yield after $ClONO_2$ hydrolysis on ice held at 173 K for various $ClONO_2$ exposures between 0.1 and 2.0 langmuirs. The solid line is the best fit to a Langmuirian isotherm of the form $cx/(1 + cx)$. (B) Rates for the $ClONO_2$ hydrolysis reaction obtained for various $ClONO_2$ exposures between 0.1 and 2.0 langmuirs. The ice was held at 173 K.

$$[P](t) = \frac{[A_o] + [P_o]}{1 + \left(\frac{[A_o]}{[P_o]}\right)e^{-k([A_o]+[P_o])t}} \quad (6)$$

Here, the subscript o indicates the initial surface concentrations of reactant A and autocatalyst P, and the equality $[A_o] - [A] = [P] - [P_o]$ was used to arrive at eq 6. Comparison with eq 5 reveals that the fit parameter r is the reaction rate given by $k([A_o] + [P_o])$, where k is the autocatalytic rate constant. Use of eq 5 as a fit function yields reliable reaction rates r, and knowledge of the absolute reactant surface concentrations is not required.

An alternative explanation for the data could be offered that an intermediate invisible to our laser system is formed during the hydrolysis reaction of $ClONO_2$, according to $A + B \xrightarrow{k_f} C \xrightarrow{k_d} D + E$. However, the rate of the intermediate formation and its decay to D and E should not be influenced when the system is preconditioned with product molecules D or E. The observation that the induction times are shortened considerably when the $ClONO_2$ hydrolysis is carried out on ice surfaces preconditioned with HOCl is not consistent with two consecutive reactions involving an intermediate.

It could also be argued that the observed surface kinetics are due to surface or bulk diffusion. The observed dosing effects could be the result of the dosed molecules affecting the diffusion

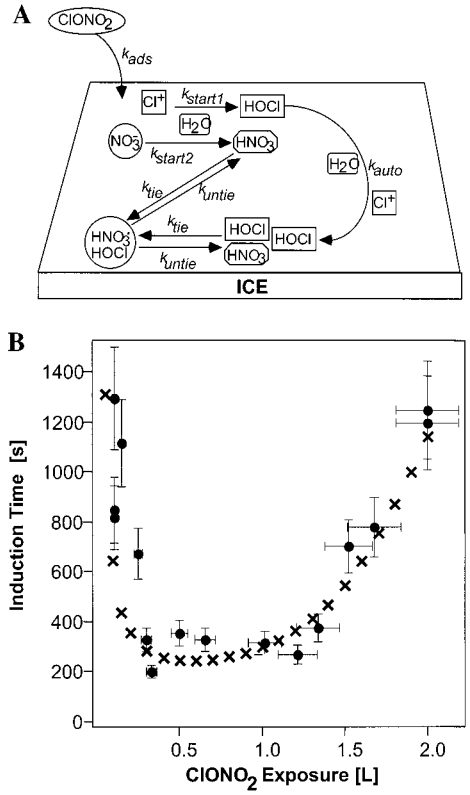

Figure 4. (A) Proposed kinetic scheme of the autocatalytic step involved in the heterogeneous $ClONO_2$ hydrolysis reaction on ice. (B) Comparison of the calculated (×) and measured (filled circles) induction times for the heterogeneous $ClONO_2$ hydrolysis reaction on ice. The parameter values used in the model are listed in Table 1.

of reactants in some way. Measuring the induction times for low (0.3 langmuir) $ClONO_2$ exposures for ice crystal temperatures between 163 and 188 K, we find that they are temperature independent with an average value of 300 ± 200 s. The temperature independence of the induction times would not be consistent with diffusive processes, which usually have energy barriers.[33] The temperature variation experiment also argues against the postulate that the observed surface signals are the result of time-dependent reorientations of the HOCl product molecule: reorientation processes, which could affect SHG signal intensities, are expected to have energy barriers as well. Experiments using 45° polarized light input and collecting all polarizations of the SHG signal showed intensity vs time traces similar to those in Figure 1. Thus, the observed SHG signals from the $ClONO_2$-dosed ice surface are not very sensitive to the tensorial properties of SHG.

4. Discussion

On the basis of the experimental results presented in this work and ab initio calculations by Bianco and Hynes[31] and Xu and Zhao,[32] we suggest the following reaction mechanism for the hydrolysis of $ClONO_2$ after its adsorption at the ice surface (Figure 4A):

$$nH_2O + ClONO_2(ads) \xrightarrow{k_{start}} HNO_3(ads) + HOCl(ads) + (n-1)H_2O \quad (7)$$

$$nH_2O + ClONO_2(ads) + HOCl(ads) \xrightarrow{k_{auto}} HNO_3(ads) + 2HOCl(ads) + (n-1)H_2O \quad (8)$$

For a given $ClONO_2$ exposure, the initial HOCl formation rate is slow during the starter step (reaction 7) and speeds up with time as more HOCl is formed during the autocatalytic step (reaction 8) until all $ClONO_2$ is depleted. As the surface is exposed to more $ClONO_2$, more HOCl is formed at the surface, in agreement with data in Figure 3A. Higher HOCl coverage results in a faster rate (Figure 3B); hence the induction times are shortened with increasing $ClONO_2$ exposure. These kinetic results are supported on a mechanistic level: in reaction 8, protonation of the nitrate group is easier than in reaction 7 since HOCl is a slightly better proton donor than water. The weak acidity of the autocatalyst appears to play an important role in reaction 8: in separate experiments, we observed a similar shortening of the induction times when ice surfaces were exposed to 0.1−0.5 langmuir acetic acid prior to exposure to 2.0 langmuirs $ClONO_2$. The induction time was shortened from around 1200 to 170 s.

With even higher $ClONO_2$ exposures, according to our proposed model, the HNO_3 product begins to tie up reactive water sites on the ice surface. It is known from work by Livingston and George that HNO_3 dosed on ice retards both the diffusion and desorption of water molecules on ice.[33] Likewise, we observed in previous work[24] that HOCl desorption rates from ice decrease with increasing amount of predosed HNO_3. We propose that HNO_3 acts as a molecular glue for HOCl via formation of a complex ($HOCl{\cdot}HNO_3$) (Figure 4A). In the context of the $ClONO_2$ + ice reaction, this decreases the surface concentration of free autocatalytic HOCl. Second, the strong acid HNO_3 may complex several water molecules on the ice surface which is consistent with its tendency to form hydrates near these temperature and pressure conditions.[34] With less surface water molecules available, reaction 1 should be retarded, as observed when we predose the ice with HNO_3. Both cases lead to a retardation of the $ClONO_2$ hydrolysis reaction. As a result, the rate of the reaction slows down for high $ClONO_2$ exposures (Figure 3B).

The kinetic model presented in Figure 4A was tested for plausibility using numerical integration methods.[35] In our model, $ClONO_2$ adsorbs dissociatively onto the ice; this process is governed by the rate constant for adsorption, k_{ads}, and is consistent with a lack of the SHG signal from $ClONO_2$ at the surface. HOCl and HNO_3 are then formed by hydrolysis of Cl^+ and NO_3^- in two starter steps with individual rate constants k_{start1} and k_{start2}. HOCl reacts autocatalytically with H_2O and Cl^+; this step is governed by the autocatalytic rate constant k_{auto}. HOCl can also be tied up reversibly by HNO_3; this step is governed by the forward reaction rate constant k_{tie} and the backward reaction rate constant k_{untie}. Numerical integration at the Runge−Kutta fourth-order level was employed to solve the kinetic equations for the processes displayed in Figure 4A. No appreciable deviation of results was observed for step sizes between 0.125 and 1 s. Runs were carried out over 1400 s, and $ClONO_2$ exposures between 0.1 and 2 langmuirs were achieved by coding the equivalent of an on−off valve. Variation of the $ClONO_2$ pressure and the dosing time allowed for the replication of the actual experimental conditions. The ice surface consisted of 6×10^{14} water adsorption sites. Calculation of individual HOCl concentration vs time profiles for varying amounts of $ClONO_2$ gave induction times that are in good agreement with the experimentally observed induction times (Figure 4B). (For parameters see Table 1.) The kinetic model presented in Figure 4A is therefore consistent with the physical and chemical processes we observed for the heterogeneous hydrolysis of $ClONO_2$ on ice.

TABLE 1: Parameters from the Kinetic Model Used for Calculating Induction Times for the Heterogeneous $ClONO_2$ Hydrolysis Reaction on Ice

parameter	value
k_{ads}	2.9×10^5 Torr^{-1} s^{-1}
k_{start1}	1×10^{-29} cm^2 molecules^{-1} s^{-1}
k_{start2}	1×10^{-29} cm^2 molecules^{-1} s^{-1}
k_{auto}	4.5×10^{-30} cm^4 molecules^{-2} s^{-1}
k_{tie}	7.5×10^{-16} cm^2 molecules^{-1} s^{-1}
k_{untie}	7.5×10^{-16} s^{-1}
$[H_2O]$	6×10^{14} molecules cm^{-2}

The mechanism by Bianco and Hynes provides one reason for why ice is needed for the heterogeneous $ClONO_2$ hydrolysis reaction: since half of the transition state morphology is presented to the incoming $ClONO_2$ in the form of an ice surface, the activation energy required for the hydrolysis reaction is lowered enough to allow reaction 7 to occur on ice.[31] Measuring the induction times corresponds to measuring the starter step kinetics (reaction 7). Our experimental observation that the induction times are not dependent on temperature is consistent with ab initio calculations by Bianco and Hynes that indicate a low (12 kJ/mol) energy barrier for reaction 7 with $n = 3$.[31]

This present work has shown a second important role played by the ice surface in the ozone-depleting $ClONO_2$ hydrolysis reaction: it acts as a reservoir so that the (weak) acid-catalyzed second step (reaction 8) can occur. It is this acid-catalyzed reaction that allows the efficient conversion of chlorine nitrate to HOCl and HNO_3 on ice.

The observed reaction times in this study are on the order of 100−1000 s. Given the fact that the ozone depleting reactions occur on the time scale of months during the polar night when PSC particles are present, it is clear that the chlorine nitrate hydrolysis reaction has plenty of time to occur efficiently on stratospheric ice particles. Models for stratospheric ozone depletion are insensitive to the kinetic or mechanistic details of reactions 1−3 since the reactions are not limiting the rate of the overall ozone depletion process.

It is clear from these studies that the often used γ parameter, the reaction probability, may not in fact be a constant but can change during the course of a reaction since the surface composition changes due to product buildup, and the products can modify the reactions rates.

5. Summary

In this study, we find that the reaction mechanism of the $ClONO_2$ hydrolysis on ice is autocatalytic in nature and that HOCl acts as the autocatalyst, while the HNO_3 coproduct delays the reaction. Thus, the reaction of $ClONO_2$ on the equilibrium basal ice surface at 185 K is unusual in that one of the products HOCl is a catalyst and the other product HNO_3 is an inhibitor. The ice surface plays a dual role by (1) presenting an array of water molecules that help form the reaction transition state in a first step and (2) serving as a reservoir so that the reaction can be catalyzed by HOCl, the weak acid product, in a second step. Sum frequency generation experiments that give vibrational information about surface species[21] will be of great utility in further characterizing reactions on ice, including addressing interesting questions regarding ionization of species at the interface.

Acknowledgment. We acknowledge the support of NSF grant ATM 9022613 and the Presidential Young Investigator Award ATM-9158080. J.M.H. thanks the Henry B. Luce Foundation and the Alfred P. Sloan Foundation for support.

F.M.G. thanks NASA for a Global Change Graduate Student Fellowship in Earth System Sciences.

References and Notes

(1) Molina, M. J.; Rowland, F. S. *Nature* **1974**, *249*, 810−812.
(2) Solomon, S.; Garcia, R. R.; Rowland, F. S.; Wuebbles, D. J. *Nature* **1986**, *321*, 755−758.
(3) Crutzen, P. J.; Arnold, F. *Nature* **1986**, *324*, 651.
(4) Tolbert, M. A.; Rossi, M. J.; Malhotra, R.; Golden, D. M. *Science* **1987**, *238*, 1258−1260.
(5) Molina, M. J.; Tso, T.-L.; Molina, L. T.; F. Wang, C.-Y. *Science* **1987**, *238*, 1253−1257.
(6) Douglass, A. R.; Stolarski, R. S. *Geophys. Res. Lett.* **1989**, *16*, 131−134.
(7) Carslaw, K. S.; Mulvaney, R.; Oates, K. *Geophys. Res. Lett.* **1989**, *16*, 487.
(8) Toon, O. B.; Hamill, P.; Turco, R.; Pinto, J. *Geophys. Res. Lett.* **1986**, *13*, 1284−1287.
(9) Pueschel, R. F.; et al. *J. Geophys. Res.* **1989**, *94*, 16449.
(10) Baker, M. B.; Dash, J. G. *J. Geophys. Res.* **1996**, *101*, D8, 12929−12931.
(11) Fletcher, N. H. *The Chemical Physics of Ice*; Cambridge University Press: Cambridge, U.K., 1970.
(12) Hanson, D. R.; Ravishankara, A. R. *J. Phys. Chem.* **1993**, *97*, 12309−12319.
(13) Molina, M. J.; et al. *Science* **1993**, *261*, 1418−1423.
(14) Zhang, R.; Leu, M.-L.; Keyser, L. F. *J. Phys. Chem.* **1994**, *98*, 13563−13574.
(15) Lee, S.-H.; Leard, D. C.; Zhang, R.; Molina, L. T.; Molina, M. J. *Chem. Phys. Lett.* **1999**, *315*, 7−11.
(16) Tolbert, M. A.; Rossi, M. J.; Golden, D. M. *Science* **1988**, *240*, 1018−1021.
(17) Oppliger, R.; Allanic, A.; Rossi, M. J. *J. Phys. Chem. A* **1997**, *101*, 1903−1911.
(18) Berland, B. S.; Tolbert, M. A.; George, S. M. *J. Phys. Chem. A* **1997**, *101*, 9954−9963.
(19) Hanson, D. R. *J. Phys. Chem. B* **1997**, *101*, 4998.
(20) *Chemical Kinetics and Photochemical Data for Use In Stratospheric Modeling, Evaluation no. 12*; JPL Publication: Pasadena, California, Jan 15, 1997.
(21) Shen, Y. R. *The Principles of Nonlinear Optics*; John Wiley & Sons: New York, 1984.
(22) Eisenthal, K. B. *Chem. Rev.* **1996**, *96*, 1343−1360.
(23) Geiger, F. M.; J. M. Hicks *Laser Techniques in Surface Science*; SPIE: Bellingham, WA, 1998; Vol. 3272, pp 296−302.
(24) Geiger, F. M.; Tridico, A. C.; Hicks, J. M. *J. Phys. Chem. B* **1999**, *103*, 8205−8215.
(25) Tridico, A. C.; Lakin, M.; Hicks, J. M. *Laser Techniques in Surface Science*; SPIE: Bellingham, WA, 1998; Vol. 2125, pp 160−171.
(26) Wong, T. M.; Tridico, A. C.; Miller, L. M.; Hicks, J. M. In *Physics and Chemistry of Ice*; Maeno, N., Hondoh, T., Eds.; Hokkaido University Press: Sapporo, 1992; pp 190−193.
(27) Marti, J.; Mauersberger, K. *Geophys. Res. Lett.* **1993**, *20*, 363−366.
(28) McNamara, J. P.; Hillier, I. H. *J. Phys. Chem. A* **1999**, *103*, 7310−7321.
(29) Banham, S. F.; Horn, A. B.; Koch, T. G.; Sodeau, J. R. *Faraday Discuss.* **1995**, *100*, 321−332.
(30) Steinfeld, J. I.; Francisco, J. S.; Hase, W. L. *Chemical Kinetics and Dynamics*; Prentice Hall: Englewood Cliffs, New Jersey, 1989.
(31) Bianco, R.; Hynes, J. T. *J. Phys. Chem. A* **1998**, *102*, 309−314.
(32) Xu, S. C.; Zhao, X. S. *J. Phys. Chem. A* **1999**, *103*, 2100−2106.
(33) Livingston, F. E.; George, S. M. *J. Phys. Chem. B* **1999**, *103*, 4366−4376.
(34) Worsnop, D. R.; Fox, L. E.; Zahniser, M. S.; Wofsy, S. C. *Science* **1993**, *259*, 71−74.
(35) Liu, W.; et al. Stella Research: High Performance Systems, Inc., Hanover, NH 03755, 1997.